Kondo physics in the single-electron transistor with ac driving

Peter Nordlander
Department of Physics and Rice Quantum Institute, Rice University, Houston, Texas 77251-1892

Ned S. Wingreen
NEC Research Institute, 4 Independence Way, Princeton, New Jersey 08540

Yigal Meir
Physics Department, Ben Gurion University, Beer Sheva, 84105, Israel

David C. Langreth
Center for Materials Theory, Department of Physics and Astronomy, Rutgers University, Piscataway, New Jersey 08854-8019
(Received 20 September 1999)

Using a time-dependent Anderson Hamiltonian, a quantum dot with an ac voltage applied to a nearby gate is investigated. A rich dependence of the linear response conductance on the external frequency and driving amplitude is demonstrated. At low frequencies a sufficiently strong ac potential produces sidebands of the Kondo peak in the spectral density of the dot, and a slow, roughly logarithmic decrease in conductance over several decades of frequency. At intermediate frequencies, the conductance of the dot displays an oscillatory behavior due to the appearance of Kondo resonances of the satellites of the dot level. At high frequencies, the conductance of the dot can vary rapidly due to the interplay between photon-assisted tunneling and the Kondo resonance.

It has been predicted that at low temperatures, transport through a quantum dot should be governed by the same many-body phenomenon that enhances the resistivity of a metal containing magnetic impurities—namely, the Kondo effect.[1,2] The recent observations of the Kondo effect[3] in a quantum dot operating as a single-electron transistor (SET) have fully verified these predictions. In contrast to bulk metals, where the Kondo effect corresponds to the screening of the free spins of a large number of magnetic impurities, there is only one free spin in the quantum-dot experiment. Moreover, a combination of bias and gate voltages allow the Kondo regime, mixed-valence regime, and empty-site regime all to be studied for the same quantum dot, both in and out of equilibrium.[3]

Here we consider another opportunity presented by the observation of the Kondo effect in a quantum dot that is not available in bulk metals—the application of an unscreened ac potential. There is already a large literature concerning the experimental application of time-dependent fields to quantum dots.[4] For a dot acting as a Kondo system, the ac voltage can be used to periodically modify the Kondo temperature or to alternate between the Kondo and mixed-valence regimes. Thus it is natural to ask what additional phenomena occur in a driven system which in steady state is dominated by the Kondo effect. Hettler and Schoeller (HS)[5] addressed this question within the framework of the Anderson model with an ac potential of frequency Ω applied to the dot. They reported that, in addition to the Kondo peak at the Fermi energy, the density of states of the dot developed sidebands spaced by $\hbar\Omega$. As we show later, for the parameters HS studied, the correct NCA equations *do not* produce sidebands. However sidebands do appear with stronger ac driving of the dot. Other works have addressed the response of an impurity of the Kondo[6] or Anderson[7] type to an ac *bias* applied between the two leads. Since a bias voltage produces Kondo peaks at the chemical potential of each lead,[2] a small ac bias amplitude, of order T_K/e, is sufficient to spawn sidebands of the Kondo peak.[6,7]

Here we reconsider the problem of an ac potential applied to a quantum dot without ac bias between the leads. Our results indicate a rich range of behavior with increasing ac frequency, from sidebands of the Kondo peak at low ac frequencies, to conductance oscillations at intermediate frequencies, and finally to photon-assisted tunneling at high ac frequencies. Finally, by mapping the ac Anderson model to an ac Kondo model, we provide an analytic expression for strength of the ac sidebands of the Kondo peak.

The system of interest is a semiconductor quantum dot, as pictured schematically in Fig. 1. An electron can be constrained between two reservoirs by tunneling barriers leading to a virtual electronic level within the dot at energy $\sim \epsilon_{\mathrm{dot}}$

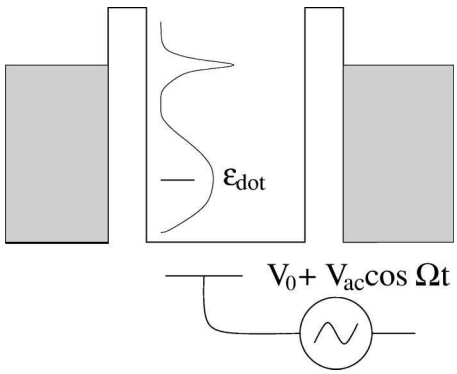

FIG. 1. Schematic picture of the quantum dot SET.

 ©2000 The American Physical Society

(measured from the Fermi level) and width $\sim 2\Gamma_{\rm dot}$.[8] We assume that both the charging energy e^2/C and the level spacing in the dot are much larger than $\Gamma_{\rm dot}$, so the dot will operate as a SET.[4] In this work, we consider only the linear-response conductance between the two reservoirs. However, we will allow an oscillating gate voltage $V_g(t)=V_0+V_{\rm ac}\cos\Omega t$ of arbitrary (angular) frequency Ω and arbitrary amplitude $V_{\rm ac}$, which modulates the virtual-level energy $\epsilon_{\rm dot}(t)$.

Such a system may be described by a constrained ($U=\infty$) Anderson Hamiltonian

$$\sum_\sigma \epsilon_{\rm dot}(t) n_\sigma + \sum_{k\sigma} [\epsilon_{k\sigma} n_{k\sigma} + (V_k c^\dagger_{k\sigma} c_\sigma + \text{H.c.})]. \quad (1)$$

Here $c^\dagger_\sigma$ creates an electron of spin σ in the quantum dot, while n_σ is the corresponding number operator; $c^\dagger_{k\sigma}$ creates a corresponding reservoir electron; k is shorthand for all other quantum numbers of the reservoir electrons, including the designation of left or right reservoir, while V_k is the tunneling matrix element through the appropriate barrier. Because the charging energy to add a second electron, $U=e^2/C$, is assumed large, the Fock space in which the Hamiltonian (1) operates is restricted to those elements with zero or one electron in the dot.

At low temperatures, the Anderson Hamiltonian (1) gives rise to the Kondo effect when the level energy $\epsilon_{\rm dot}$ lies below the Fermi energy. In this regime, a single electron occupies the dot which, in effect, turns the dot into a magnetic impurity with a free spin. The temperature required to observe the Kondo effect in linear response is of order $T_K \sim D\exp(-\pi|\epsilon_{\rm dot}|/\Gamma_{\rm dot})$, where D is the energy difference between the Fermi level and the bottom of the band of states. For the temperature range that is likely to be experimentally accessible in a SET, $T\sim T_K$ or higher, there exists a well tested and reliable approximation known as the noncrossing approximation (NCA).[9] The NCA has been formally generalized to the full time-dependent nonequilibrium case,[10] and a method for its numerical solution was proposed and implemented.[11] Here we present the full numerical solution of the time-dependent NCA equations without additional approximation, as applied to a quantum dot over the full range of applied frequencies.

The time-dependent electronic structure of the dot can be characterized by the time-dependent spectral density

$$\rho_{\rm dot}(\epsilon,t) \equiv \int_{-\infty}^{\infty} \frac{d\tau}{2\pi} e^{i\epsilon\tau/\hbar} \langle \{ c_\sigma(t+\tfrac{1}{2}\tau), c^\dagger_\sigma(t-\tfrac{1}{2}\tau) \} \rangle \quad (2)$$

evaluated in the restricted Fock space. For the equilibrium Kondo system, $\rho_{\rm dot}(\epsilon)$ is time independent, and looks similar to the graph in the schematic in Fig. 1. Roughly speaking, $\rho_{\rm dot}(\epsilon)$ consists of a broad peak of width $\sim 2\Gamma_{\rm dot}$ at the level position $\epsilon_{\rm dot}$ and a sharp Kondo peak of width $\sim T_K$ near the Fermi level. We will refer to these features as the virtual-level peak and the Kondo peak, respectively. In the steady-state case, the linear-response conductance G through a dot symmetrically coupled to two reservoirs is given by[12]

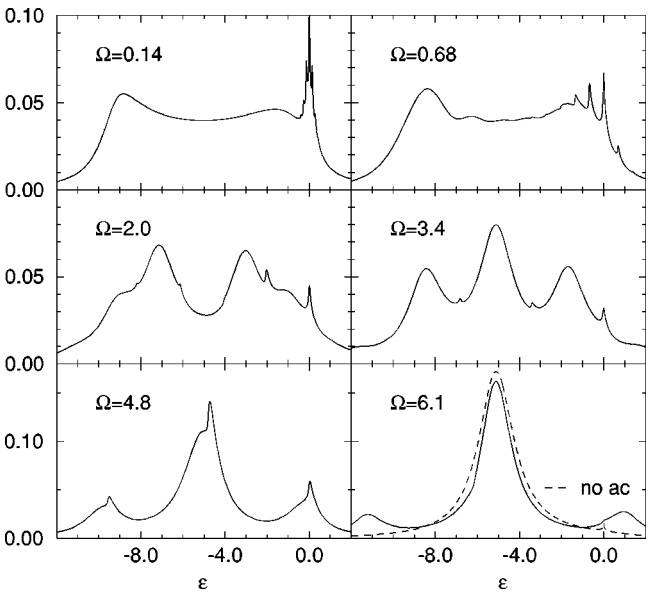

FIG. 2. The spectral density $\langle \rho_{\rm dot}(\epsilon,t) \rangle$ vs energy ϵ for a quantum dot with level energy $\epsilon_{\rm dot}(t) = -5 + 4\cos\Omega t$ and $T=0.005$. The nondriven case is also shown in the final panel. Throughout this letter, energies are in units of $\Gamma_{\rm dot}$.

$$G = \frac{e^2}{\hbar}\frac{\Gamma_{\rm dot}}{2}\int d\epsilon \rho_{\rm dot}(\epsilon)\left(-\frac{\partial f(\epsilon)}{\partial \epsilon}\right), \quad (3)$$

where $f(\epsilon)$ is the Fermi function. The formula (3) will still be valid in the case where the gate voltage is time dependent if G is the *time-averaged* conductance and $\rho_{\rm dot}(\epsilon)$ is replaced by the *time-averaged* spectral density $\langle \rho_{\rm dot}(\epsilon,t) \rangle$.[13,14] For a given system, this average will depend on the driving amplitude $V_{\rm ac}$ and frequency Ω.

In Fig. 2 we show the calculated $\langle \rho_{\rm dot}(\epsilon,t) \rangle$ as a function of energy ϵ for a level with energy $\epsilon_{\rm dot}(t) = \epsilon_{\rm dot} + \epsilon_{\rm ac}\cos\Omega t$ at several different frequencies Ω. The corresponding conductance is shown by the curve labeled dot A, $T=0.005$ in Fig. 3. For the lowest Ω, the response of the system is relatively adiabatic and the displayed spectral function resembles the spectral function that would have resulted if the system had been in perfect equilibrium for all the dot level positions over a period of oscillation of $\epsilon_{\rm dot}(t)$. The two broad peaks are the influence of the virtual level peaks at the two stationary points of this oscillation (here at $\epsilon=-1$ and $\epsilon=-9$). As the frequency Ω is increased, marked nonadiabatic effects result, the most obvious being the appearance of multiple satellites around the Kondo resonance. These sidebands appear at energies equal to $\hbar$ times multiples of the driving frequency Ω.[15] With increasing frequency, the magnitude of the Kondo peak at the Fermi energy also declines. This in turn causes the slow, roughly logarithmic falloff of the conductance over two decades of frequency, as shown in Fig. 3. In a recent work, Kaminski, Nazarov, and Glazman[16] have attributed the decay of the Kondo peak observed here to decoherence induced by ac excitations. Such a mechanism was originally proposed[2] to explain the reduction of the Kondo peak amplitude under application of a dc bias. As we will show, the same mechanism also applies to reduce the Kondo peak amplitude at high ac frequencies $\hbar\Omega \gg \Gamma_{\rm dot}$.

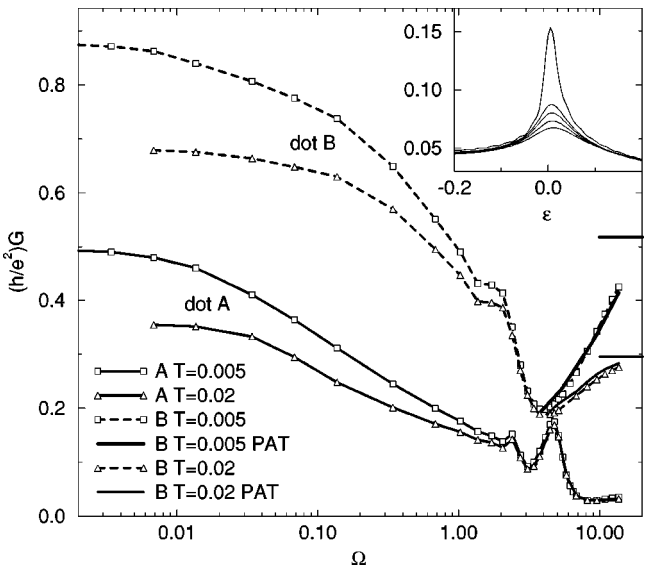

FIG. 3. Conductance of two different quantum dots, each at two different temperatures: Dot A, $\epsilon_{\rm dot}(t) = -5 + 4\cos\Omega t$; dot B, $\epsilon_{\rm dot}(t) = -2.5 + 2\cos\Omega t$. The curves at the high Ω end for dot B (marked ''PAT'') are from our photon-assisted-tunneling model, while the exact high frequency asymptotes for dot B are shown as short horizontal lines extending from the right vertical axis. The inset shows the spectral density $\langle \rho_{\rm dot}(\epsilon,t)\rangle$ of dot B around the Fermi level, at $T=0.005$, for large frequencies, from $\Omega=4.8$ (lowest curve), through 5.5, 6.1, 6.8 to $\Omega=14$ (topmost curve).

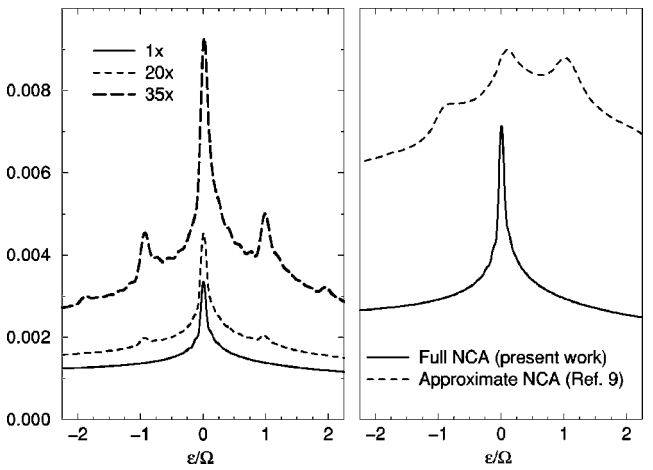

FIG. 4. Left panel: Evolution of the Kondo sidebands in the spectral weight vs ac driving. Right panel: Direct comparison with Ref. 5 (vertical scales and offsets arbitrary) for the weakest driving ($1\times$) used there.

As $\hbar\Omega$ becomes larger than $\Gamma_{\rm dot}$, inspection of Fig. 2 shows that broad satellites also appear at energy separations $n\hbar\Omega$ around the average virtual-level position $\epsilon_{\rm dot}$. These satellites of the virtual level are the analogs of those predicted in the noninteracting case,[13] which decrease in magnitude as the order n of the squared Bessel function $[J_n(\epsilon_{\rm ac}/\hbar\Omega)]^2$. Here, however, the virtual-level satellites have their own Kondo peaks; each of the latter gets strong when the corresponding virtual-level satellite reaches a position a little below the Fermi level, and then disappears as the broad satellite crosses the Fermi level. This effect produces the oscillations in the conductance that are evident in the lower curves in Fig. 3. These oscillations are very different from those that would occur in a noninteracting ($U=0$) case: due to the Kondo peaks they are substantially stronger, their maxima occur at different frequencies and their magnitudes are temperature dependent.

As the last virtual-level satellite crosses the Fermi level, $\hbar\Omega = |\epsilon_{\rm dot}|$, the dot level energy begins to vary too fast for the system to respond and the average spectral function approaches the *equilibrium* spectral function for a dot level centered at the average position $\epsilon_{\rm dot}$. Indeed, in the limit $\Omega\to\infty$ the time-averaged spectral function is exactly equal to the equilibrium spectral function centered at $\epsilon_{\rm dot}$. For the parameters of Fig. 2, this very high frequency region is uninteresting, because for $\epsilon_{\rm dot}=-5$ the temperature $T=0.005$ is far above the Kondo temperature ($\sim 10^{-7}$). Therefore, the conductance shows little temperature or frequency dependence for $\Omega>7$.

The situation is quite different for the system (dot B) displayed in the upper two curves in Fig. 3, which displays a strong Kondo effect ($T_{\rm K}\sim 10^{-3}$) when the dot level is held at its average energy $\epsilon_{\rm dot}$. In this case the $\Omega\to\infty$ conductance is strongly enhanced by the Kondo effect, and is consequently temperature dependent as well. Note that the conductance is significantly lower than its asymptotic, $\Omega\to\infty$, value for frequencies still much larger than either the depth of the level $|\epsilon_{\rm dot}|$ or its width. This effect is due to an efficient suppression of the amplitude of the Kondo peak in the spectral density, as illustrated in the inset of Fig. 3. We propose the following explanation for this phenomenon. The energy $\hbar\Omega$ excites the dot, producing satellites[13,17] of the virtual level peak at energies $\epsilon_{\rm dot}\pm n\hbar\Omega$, which, for $\hbar\Omega \gg \Gamma_{\rm dot}$ have strength roughly given by $[J_n(\epsilon_{\rm ac}/\hbar\Omega)]^2$ as in the $U=0$ case (see Fig. 2 and the previous discussion). For large $\hbar\Omega$, only the two $n=1$ satellites have any significant strength, and the higher lies above the Fermi level, allowing an electron on the dot to decay at the rate $(1/\hbar)\Gamma_{\rm dot}(\epsilon_{\rm dot}+\hbar\Omega)$. The overall electron decay probability per unit time $\Gamma_{\rm decay}/\hbar$ due to this photon-assisted-tunneling mechanism (PAT) is therefore given by

$$\Gamma_{\rm decay} \approx [J_1(\epsilon_{\rm ac}/\hbar\Omega)]^2 \Gamma_{\rm dot}(\epsilon_{\rm dot}+\hbar\Omega). \tag{4}$$

The above rate carries with it an energy uncertainty, which we speculate has roughly the same effect on the Kondo peak as the energy smearing due to a finite temperature. We can test this conjecture by calculating the *equilibrium* conductance at an *effective* temperature $T_{\rm eff}$ given by $T_{\rm eff}=T+\Gamma_{\rm decay}$. The results of such a calculation are shown in Fig. 3 (PAT curves), where they compare very favorably with our results for the conductance in the ac-driven system.

An important conclusion of our study is that the effects of ac driving of the level energy become become significant only when $\epsilon_{\rm ac}$ becomes comparable to the ''large'' energy parameters $|\epsilon_{\rm dot}|$ and $\Gamma_{\rm dot}$; an $\epsilon_{\rm ac}\sim T_{\rm K}$ has essentially no effect.[18] This is in contrast to the the predictions of Ref. 5, where a further approximation to the NCA equations was introduced. To demonstrate the unphysical consequences of this approximation, we have used the exact parameters used in Ref. 5. The left panel of Fig. 4 shows our predicted spectral functions in the region of the Kondo resonance. The curve marked ''$1\times$'' is for the same value of driving $\epsilon_{\rm ac}$ as

Fig. 1 of Ref. 5, that is $\epsilon_{ac}=0.017|\epsilon_{dot}|=1.4\Omega=22T_K$. The curves marked $20\times$ and $35\times$ correspond to driving amplitudes 20 and 35 times this, respectively. The right panel shows a direct comparison between the full NCA prediction and the approximation to the NCA made in Ref. 5. Indeed, there is no splitting of the Kondo peak for an $\epsilon_{ac}\sim T_K$.

The strengths of the the Kondo sidebands in the left panel of Fig. 4 are roughly consistent with an $(\epsilon_{ac}/\epsilon_{dot})^2$ proportionality. Such a dependence can in fact be derived analytically for the special case where the tunneling coupling V_k is sufficiently weak that it may be treated perturbatively. This is most easily done with the corresponding Kondo Hamiltonian[19]

$$\sum_{kk'\sigma\sigma'} J_{kk'}(t)\left(\vec{S}\cdot\vec{\sigma}_{\sigma\sigma'}+\frac{1}{2}\delta_{\sigma\sigma'}\right)c^{\dagger}_{k\sigma}c_{k'\sigma'}, \tag{5}$$

where the dot is replaced simply by a dynamical Heisenberg spin $\vec{S}(S^2=\frac{3}{4})$, and where the components of $\vec{\sigma}$ are the Pauli spin matrices. For near Fermi level properties we can suppress the detailed k dependence of J and V and introduce a large energy cutoff D. In the $U=\infty$ case we consider, $J(t)=|V^2/\epsilon_{dot}(t)|$.[19]

In the Kondo model, there is no quantity directly corresponding to the time-averaged density of states of the dot electron $\langle\rho_{dot}(\epsilon,t)\rangle$. Therefore, in order to use the Kondo Hamiltonian (5) to determine the strength of the sidebands in $\langle\rho_{dot}(\epsilon,t)\rangle$, we must first relate the density of states to the scattering rate of electrons in the leads. Specifically, we let $w_{leads}(\epsilon)/\hbar$ be the total rate at which lead electrons of energy ϵ undergo intralead and interlead scattering by the dot. In the Kondo regime, $w_{leads}(\epsilon)$ will have a peak for ϵ near the Fermi level. Furthermore, if J is modulated as $J(t)=\langle J\rangle(1+\alpha\cos\Omega t)$, then an electron scattered by the dot will be able to absorb or emit multiple quanta of energy $\hbar\Omega$, leading to satellites of the Kondo peak in $w_{leads}(\epsilon)$. We can then obtain $\langle\rho_{dot}(\epsilon,t)\rangle$ through the exact Anderson model relation[20]

$$\langle\rho_{dot}(\epsilon,t)\rangle=\rho_{leads}(\epsilon)w_{leads}(\epsilon)/\Gamma_{dot}(\epsilon), \tag{6}$$

where $\rho_{leads}(\epsilon)$ is the state density per spin in the leads.

We expand perturbatively in J, keeping all terms of order J^2 and logarithmic terms to order J^3, obtaining

$$w_{leads}(\epsilon)=2\pi\langle J^2\rangle\rho\left[1+3\langle J\rangle\rho\sum_{n=-1}^{1}a_n g(\epsilon+n\hbar\Omega)\right], \tag{7}$$

where $\rho=\rho_{leads}(0)$, $a_0=1$, $a_{\pm1}=\alpha^2/(2+\alpha^2)$, $\langle J^2\rangle=(1+\frac{1}{2}\alpha^2)\langle J\rangle^2$, and

$$g(\epsilon)=\frac{1}{2}\int_{-D}^{D}d\epsilon'\frac{1-2f(\epsilon')}{\epsilon'-\epsilon}\rightarrow\ln\left|\frac{D}{\epsilon}\right|, \tag{8}$$

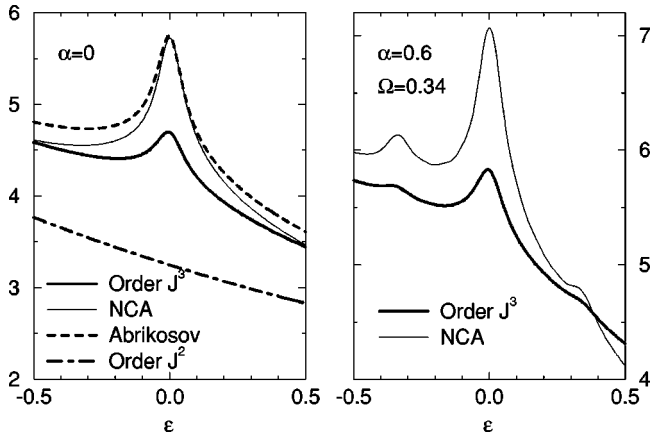

FIG. 5. Spectral density $\langle\rho_{dot}(\epsilon,t)\rangle$ times 10^3 in the Kondo model and NCA for $k_BT=0.02$ and $\langle J\rangle\rho=0.023$ ($\epsilon_{dot}=-7$). For the nondriven case (left panel) we also show the comparable result from summing all the leading logarithmic terms (Abrikosov, Ref. 21), as well as that obtained to order J^2. The energy dependence of $\langle J\rangle$ (Ref. 19) has been included to order J^2 in all the Kondo Hamiltonian curves.

the last limit being approached when $T\ll|\epsilon|$. The quantities $\alpha_{\pm}=\epsilon_{ac}^2/(2\epsilon_{dot}^2+\epsilon_{ac}^2)\approx\epsilon_{ac}^2/2\epsilon_{dot}^2$ are the strengths (equal, to this order in J) of the first satellites above and below a central peak of unit strength. In Fig. 5 we compare the perturbative results in J with the full NCA theory. Although we are not strictly in the parameter region where the J^3 theory is quantitatively valid, the qualitative agreement is quite satisfactory.

The present results indicate rich behavior when an external ac potential is applied to a quantum dot in the regime where the conductance is dominated by the Kondo effect. While the time-dependent NCA method employed spans the full range of applied frequency, some additional insight has been gained into the behavior both at very low and very high frequencies. At low frequencies a time-dependent Kondo model helps explain the amplitudes of sidebands of the Kondo peak in the spectral density of the dot. At high frequencies, a cutoff of the Kondo peak due to photon-assisted tunneling processes accounts for the reduction of conductance. We hope that our work will inspire experimental investigation of these phenomena and other ramifications of ac driving applied to Kondo systems.

The work was supported in part by NSF Grant No. DMR 95-21444 and the Robert A. Welch Foundation (Rice), NSF Grant No. DMR 97-08499 and U.S. DOE Grant No. DE-FG02-99ER45970 (Rutgers), and by the US-Israeli Binational Science Foundation (BGU).

[1] L.I. Glazman and M.E. Raikh, Pis'ma Zh. Éksp. Teor. Fiz. **47**, 378 (1988) [JETP Lett. **47**, 452 (1988)]; T.K. Ng and P.A. Lee, Phys. Rev. Lett. **61**, 1768 (1988); S. Hershfield, J.H. Davies, and J.W. Wilkins, *ibid.* **67**, 3720 (1991).

[2] Y. Meir, N.S. Wingreen, and P.A. Lee, Phys. Rev. Lett. **70**, 2601 (1993); N.S. Wingreen and Y. Meir, Phys. Rev. B **49**, 11 040 (1994).

[3] D. Goldhaber-Gordon *et al.*, Nature (London) **391**, 156 (1998);

Phys. Rev. Lett. **81**, 5225 (1998); S.M. Cronenwett, T.H. Oosterkamp, and L.P. Kouwenhoven, Science **281**, 540 (1998); T. Schmid *et al.*, Phys. Rev. B **256**, 182 (1998); F. Simmel *et al.*, Phys. Rev. Lett. **83**, 804 (1999).

[4] L.P. Kouwenhoven *et al.*, in *Mesoscopic Electron Transport*, edited by L.L. Sohn, L.P. Kouwenhoven, and G. Schön (Kluwer, Netherlands, 1997).

[5] M.H. Hettler and H. Schoeller, Phys. Rev. Lett. **74**, 4907 (1995).

[6] A. Schiller and S. Hershfield, Phys. Rev. Lett. **77**, 1821 (1996).

[7] T.K. Ng, Phys. Rev. Lett. **76**, 487 (1996); Y. Goldin and Y. Avishai, *ibid.* **81**, 5394 (1998); R. Lopez *et al.*, *ibid.* **81**, 4688 (1998).

[8] $\Gamma_{\rm dot}(\epsilon) \equiv 2\pi\Sigma_k |V_k|^2 \delta(\epsilon - \epsilon_k)$ is slowly varying. $\Gamma_{\rm dot}$ with no energy specified refers to the Fermi level value.

[9] N.E. Bickers, Rev. Mod. Phys. **59**, 845 (1987).

[10] D.C. Langreth and P. Nordlander, Phys. Rev. B **43**, 2541 (1991).

[11] H. Shao, D.C. Langreth, and P. Nordlander, Phys. Rev. B **49**, 13 929 (1994).

[12] Y. Meir and N.S. Wingreen, Phys. Rev. Lett. **68**, 2512 (1992).

[13] A.-P. Jauho, N.S. Wingreen, and Y. Meir, Phys. Rev. B **50**, 5528 (1994).

[14] For the Hamiltonian (1) the time average $\langle \rho_{\rm dot}(\epsilon,t)\rangle \equiv -{\rm Im}\langle A_{\rm dot}(\epsilon,t)\rangle/\pi$, where $A_{\rm dot}(\epsilon,t)$ is the retarded and hence causal function defined in Ref. 13, Eq. (28).

[15] Hence in an experiment one may also expect peaks spaced by $\hbar\Omega$ in the differential conductance.

[16] A. Kaminski, Yu.V. Nazarov, and L.I. Glazman, Phys. Rev. Lett. **83**, 384 (1999).

[17] P.K. Tien and J.P. Gordon, Phys. Rev. **129**, 647 (1963).

[18] In contrast, an ac *bias* voltage of order T_K/e can produce significant effects such as Kondo sidebands, cf. Refs. 6,7.

[19] J.R. Schrieffer and P.A. Wolff, Phys. Rev. **149**, 491 (1966).

[20] To derive Eq. (6), we note that the full retarded propagators g for the lead electrons are given in terms of their bare values g_0 by $g = g_0 + g_0 T g_0$ with matrix multiplication implied in the time and lead quantum number k. The transition matrix T is given by $T_{kk'} = V_k V_{k'}^* A_{\rm dot}$, where $A_{\rm dot}$ is the corresponding propagator for the dot. The above two relations may be obtained directly from Eq. (1) for arbitrary U (via the equations of motion for the c's, for example). The total transition rate is then just $-2\,{\rm Im}\,T_{kk}$ from the optical theorem, which then implies for the time averaged rate $w_{\rm leads}(\epsilon) = -2|V_k|^2 {\rm Im}\langle A_{\rm dot}(\epsilon,t)\rangle$. Finally, using the relation between A and $\rho_{\rm dot}$ given in Ref. 14 and the definition of $\Gamma_{\rm dot}(\epsilon)$ given in Ref. 8, we arrive at Eq. (6).

[21] A.A. Abrikosov, Physics (N.Y.) **2**, 5 (1965).